Supplement of Atmos. Chem. Phys., 20, 181–202, 2020
https://doi.org/10.5194/acp-20-181-2020-supplement

Atmospheric Chemistry and Physics
Open Access

Supplement of

Evaluation and uncertainty investigation of the NO_2, CO and NH_3 modeling over China under the framework of MICS-Asia III

Lei Kong et al.

Correspondence to: Xiao Tang (tangxiao@mail.iap.ac.cn)

Supplementary Material

Sect. S1 Evaluations of the standard meteorological simulations

Meteorological simulations have large impacts on the simulations of atmospheric chemistry. The simulated wind speed (u-wind and v-wind), relative humidity (RH) and air temperature (T) from the standard meteorological fields were evaluated against the observations over the NCP and PRD regions. These parameters are all important factors that influences the simulations of NO_2, CO and NH_3. For example, the wind speed determines the transport of species and the air temperature influences the reaction rates of thermal chemical reactions. The RH and T also influence the thermodynamic equilibrium of gases and aerosols.

Three-hourly meteorological observations from the Integrated Surface Database (ISD) compiled by the National Oceanic and Atmospheric Administration (NOAA), U.S. (Smith et al., 2011) were used in meteorological evaluations. The observation sites used in NCP and PRD regions are shown in fig S1. Figure S2 shows the averaged time series of the simulated and observed meteorological parameters over the NCP region from January, 2010 to December, 2010. The evaluation statistics, including correlation coefficient (R), mean bias error (MBE) and root of mean square error (RMSE), were summarized in Table S2. It clearly shows that the standard meteorology simulations well captured the main features of the observed meteorological conditions in NCP throughout the year with high correlation coefficient, small biases and low errors for all meteorological parameters. Similar results could be obtained from the evaluations of meteorological conditions over the PRD region (fig. S3). These results suggested that the standard meteorological simulations can well reproduce the meteorological conditions of the NCP and PRD regions.

Sect. S2 Descriptions of the IASI measurement of NH_3 total columns

The ANNI-NH3-v2.1R-I retrieval product (Van Damme et al., 2017;Van Damme et al., 2018) was used in this study to qualitatively evaluate the modeled monthly variations of NH_3 concentrations. It is a reanalysis version of NH_3 retrievals from IASI instruments and provides the daily morning (~9:30 am local time) NH_3 total columns from year 2008 to 2016. The morning orbit was used since IASI is generally more sensitive to the atmospheric boundary layer at this time due to more favorable thermal conditions, which could provide more information on the NH_3 concentrations in the boundary layer where NH_3 is emitted. The dataset was produced by Van Damme et al., 2018 based on the conversion of hyperspectral range indices (HRIs) using an Artificial Neural Network(Whitburn et al., 2016). It uses the ERA-interim ECWMF meteorological input data rather than the operationally provided EUMETSAT IASI Level 2 (L2) data used for the standard near-real-time version, which is more coherent in time and suitable for the study of temporal variations. To facilitate comparisons, the NH_3 total columns were averaged to monthly data at 45km × 45km MICS-Asia grids.

Sect. S3 Sensitivity experiments of high-resolution simulation in the PRD region

To investigate the impacts of horizontal resolution on the simulations of gas concentrations over the PRD region, a full-year run with finer horizontal resolutions has been conducted using the NAQPMS model, which is one of the participating CTMs in MICS-Asia III. In our experiment, two nested domains with finer horizontal resolutions were added to the original modeling domain of MICS-Asia III, which are shown in Fig. S4. The first domain (D1) is identical to the modeling domain of MICS-Asia III with horizontal resolution of 45km. The second domain (D2) covers most part of southeast China with horizontal resolution of 15km. The third domain has the finest horizontal resolution (5km) which covers the PRD region and its surrounding areas. The chemical configurations of NAQPMS in each modeling domain were completely identical to those used in MICS-Asia III. Meteorological fields for each modeling domain were simulated by the WRF model version 3.4.1, same as the standard meteorological model in MICS-Asia III. The WRF configurations were also kept same as those used in the standard meteorological simulations except two additional nested domains were added (Fig. S4). The emission inventories and boundary conditions in D1 were provided by the standard input datasets of MICS-Asia III. Since MICS-Asia III only provided the 45km-resolution emission inventories and boundary conditions, the emission rates ($\mu g/m^2/s$) and boundary conditions over one model grid in D2 and D3 were simply obtained from the corresponding model grid in its parent domain. This means that although we used the finer horizontal resolutions in D2 and D3, the resolutions of emission inventories and boundary conditions in D2 and D3 were the same as those used in D1. Therefore, the horizontal resolutions were only dynamically increased in D2 and D3. The modeling results from different modeling domains were then compared with each other to investigate the dynamical impacts of horizontal resolution on the model performance.

Figure S5 shows the spatial distributions of the observed annual mean NO_2 concentrations in PRD region overlay the simulated concentrations with different horizontal resolutions. We can clearly see that the coarse modeling results (D1) cannot resolve the high spatial variability of NO_2 concentrations in the PRD region. For simulations using finer horizontal resolutions (D2 and D3), although the spatial scales of NO_2 observations can be resolved by the 15km and 5km resolutions, the modeling results still show poor performance in capturing the observed spatial variability of NO_2 concentrations, with calculated correlation coefficient only of 0.03 and 0.02, respectively (Table S3), even worse than the coarse modeling results. Similar results could be obtained from the comparisons of CO observations and simulations using different horizontal resolutions (Fig. S6). These results indicated that the poor model performance in PRD may not be attributed to the resolution of model but more related to the resolution and/or spatial allocation of emission inventories in the PRD region. These results also suggested that only increasing the resolution of model may not help improve the model performance.

Tables:

Table S1 Configurations of the standard meteorological model and different WRF-Chem models

No	Microphysics	Longwave radiation	Shortwave radiation	Boundary layer	Cumulus physics	surface physics
Standard	Lin et al. scheme	RRTMG scheme	Goddard shortwave scheme	YSU scheme	Grell 3D ensemble scheme	Unified Noah land-surface model
M7	Lin et al. scheme	RRTM scheme	Goddard shortwave	YSU scheme	Grell 3D ensemble scheme	Unified Noah land-surface model
M8	Lin et al. scheme	RRTMG scheme	RRTMG scheme	Mellor-Yamada-Janjic TKE scheme	Grell 3D ensemble scheme	Unified Noah land-surface model
M9	Lin et al. scheme	RRTMG scheme	RRTMG scheme	YSU scheme	Grell 3D ensemble scheme	Unified Noah land-surface model
M10	Goddard Cumulus Ensemble	Goddard longwave scheme	Goddard shortwave scheme	YSU scheme	Grell 3D ensemble scheme	Unified Noah land-surface model

Table S2 Evaluation metrics of the standard meteorological simulation

	NCP			PRD		
	R	MBE	RMSE	R	MBE	RMSE
temp (℃)	1.00	0.21	1.08	1.00	-0.22	0.71
RH (%)	0.97	-0.16	5.15	0.97	3.42	4.82
u-wind (m/s)	0.91	-0.08	0.63	0.82	-0.20	0.53
v-wind (m/s)	0.93	0.33	0.76	0.93	0.05	0.81

Table S3: Evaluation metrics of the simulated annual mean NO_2 and CO concentrations over the PRD region with different horizontal resolutions.

	NO_2 (ppbv)				CO (ppmv)			
	Spatial R	MBE	NMB (%)	RMSE	Spatial R	MBE	NMB (%)	RMSE
45km	0.09	2.99	13.37	10.53	0.00	-0.51	-52.85	0.57
15km	0.03	2.19	9.81	10.15	0.00	-0.54	-56.25	0.60
5km	0.02	0.58	2.59	10.23	-0.10	-0.58	-59.23	0.62

Figures:

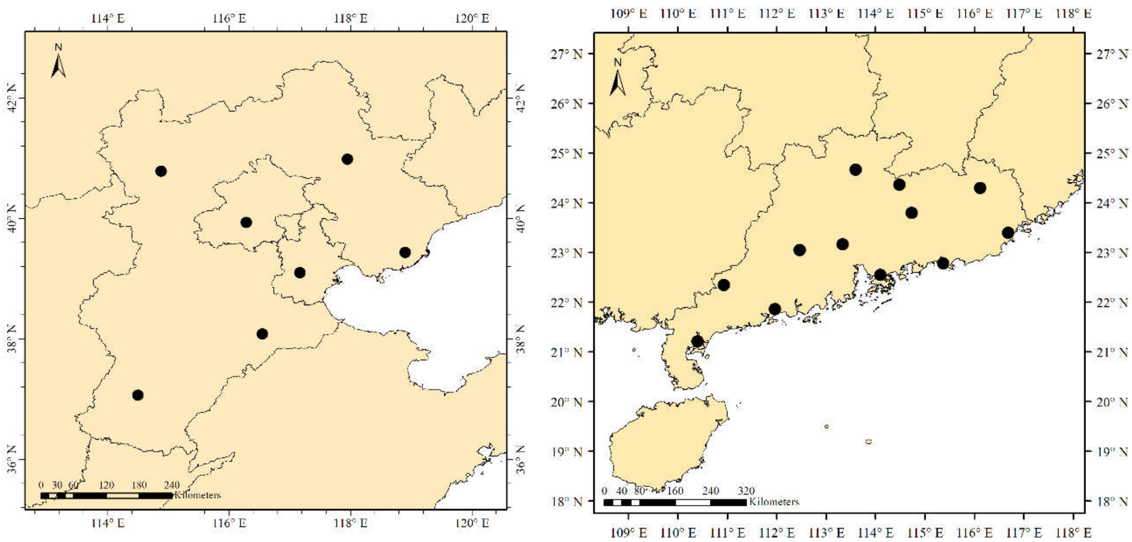

Figure S1: spatial distributions of the meteorological observation sites from the ISD over the NCP region (left panel) and the PRD region (right panel).

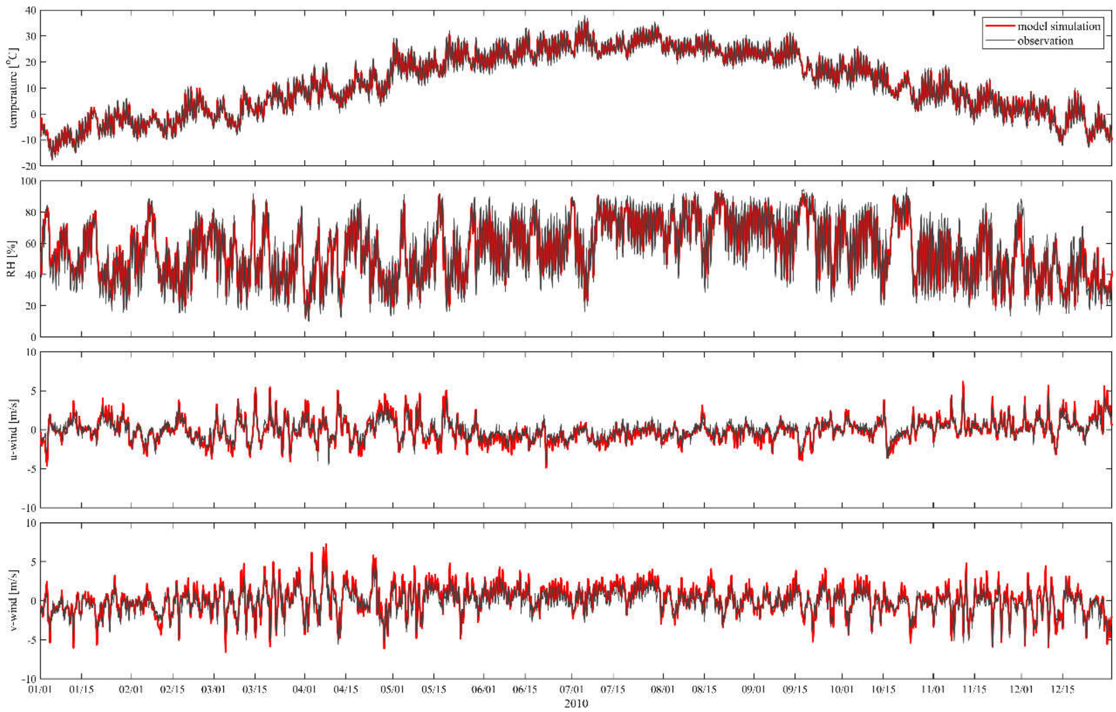

Figure S2: Time series of the simulated and observed meteorological parameters over the NCP region form January 2010 to December 2010 with an interval of three hours.

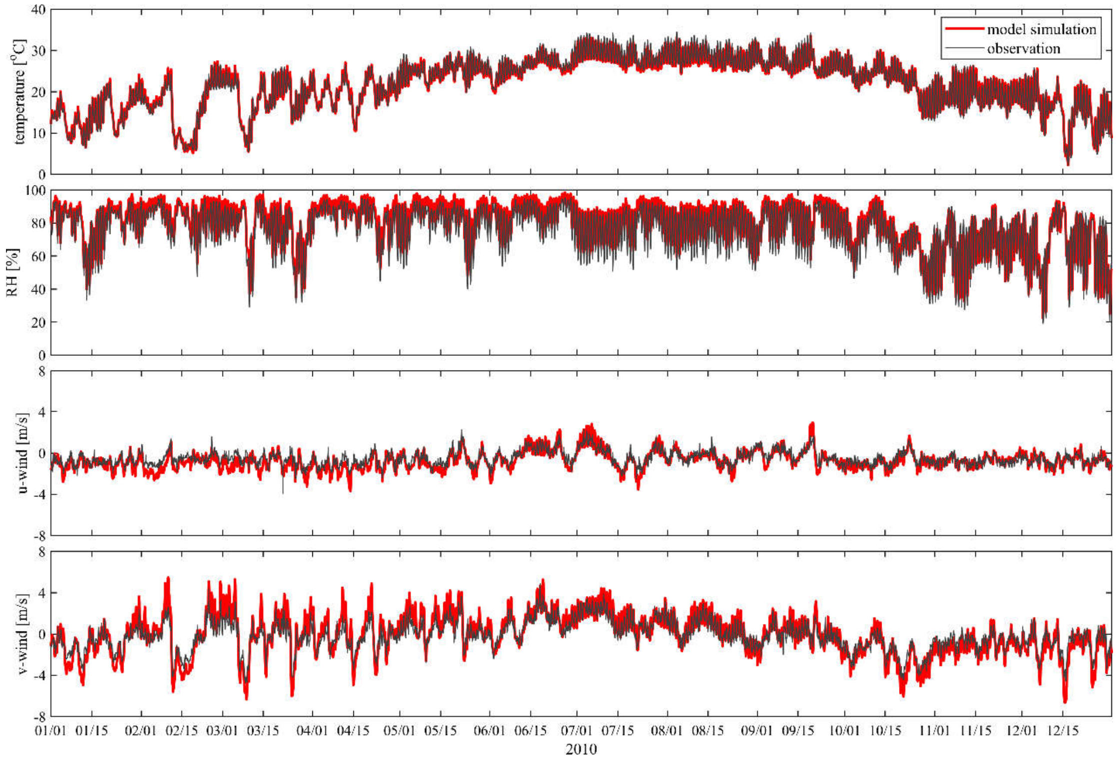

Figure S3: Same as Figure S* but for the PRD region.

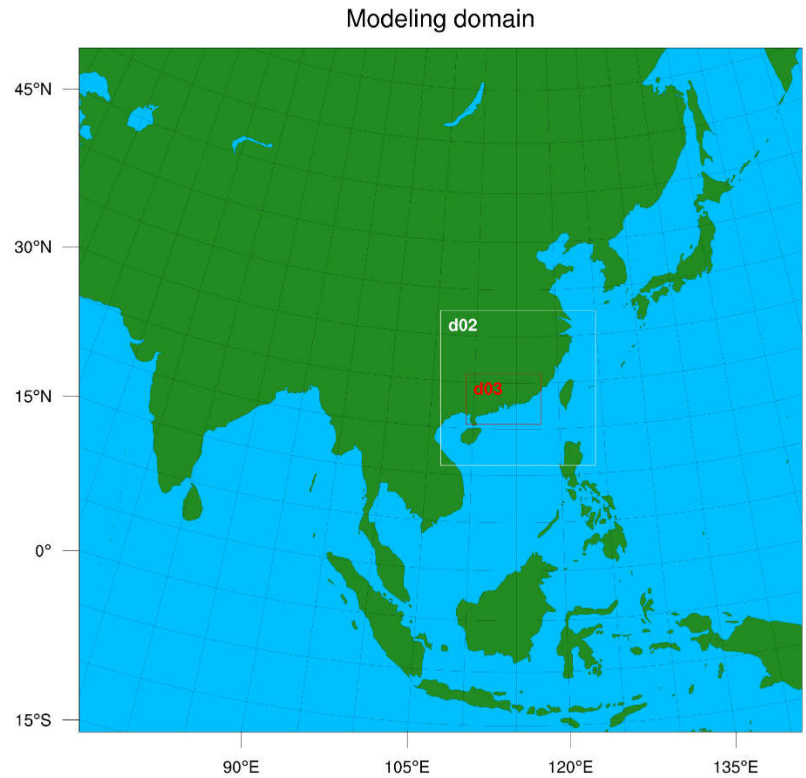

Figure S4: Modeling domain of the sensitivity experiment using different horizontal resolutions. The first domain (D1) is identical to the modeling domain of MICS-Asia III with horizontal resolution of 45km. The second domain (D2) covers most part of southeast China with horizontal resolution of 15km, and the third domain has the finest horizontal resolution (5km) covering the PRD region and its surrounding areas.

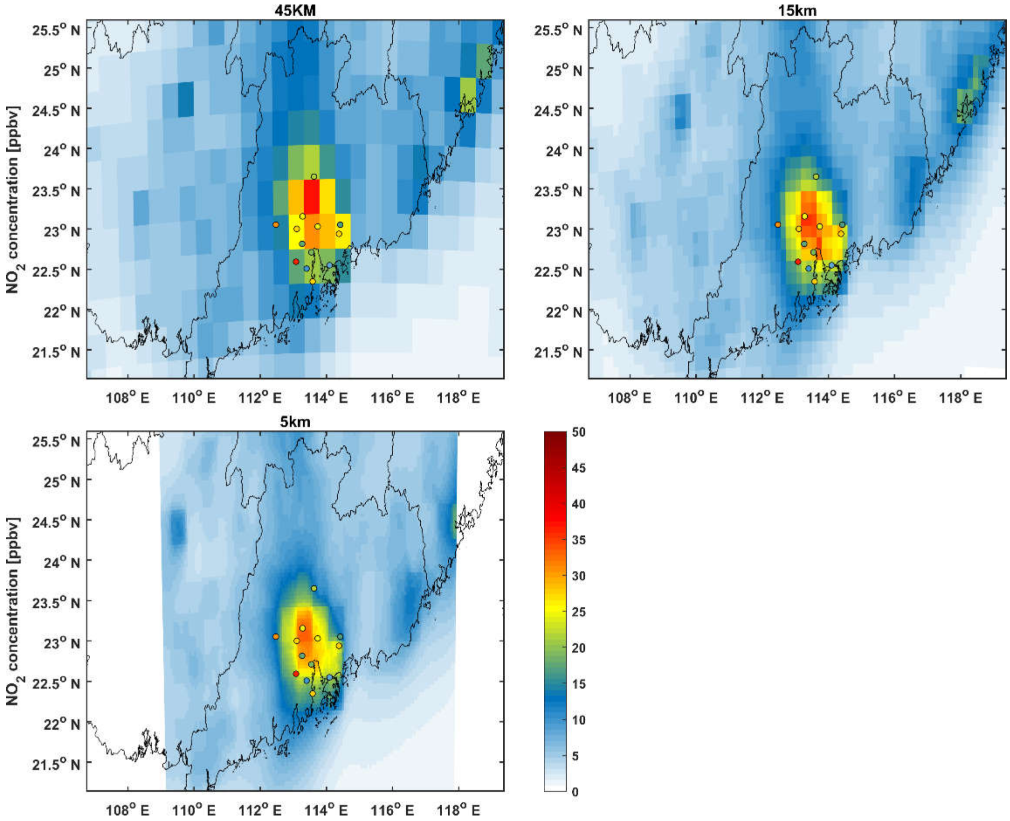

Figure S5: Spatial distributions of the observed and multi-resolution simulated annual mean NO_2 concentrations over the PRD region.

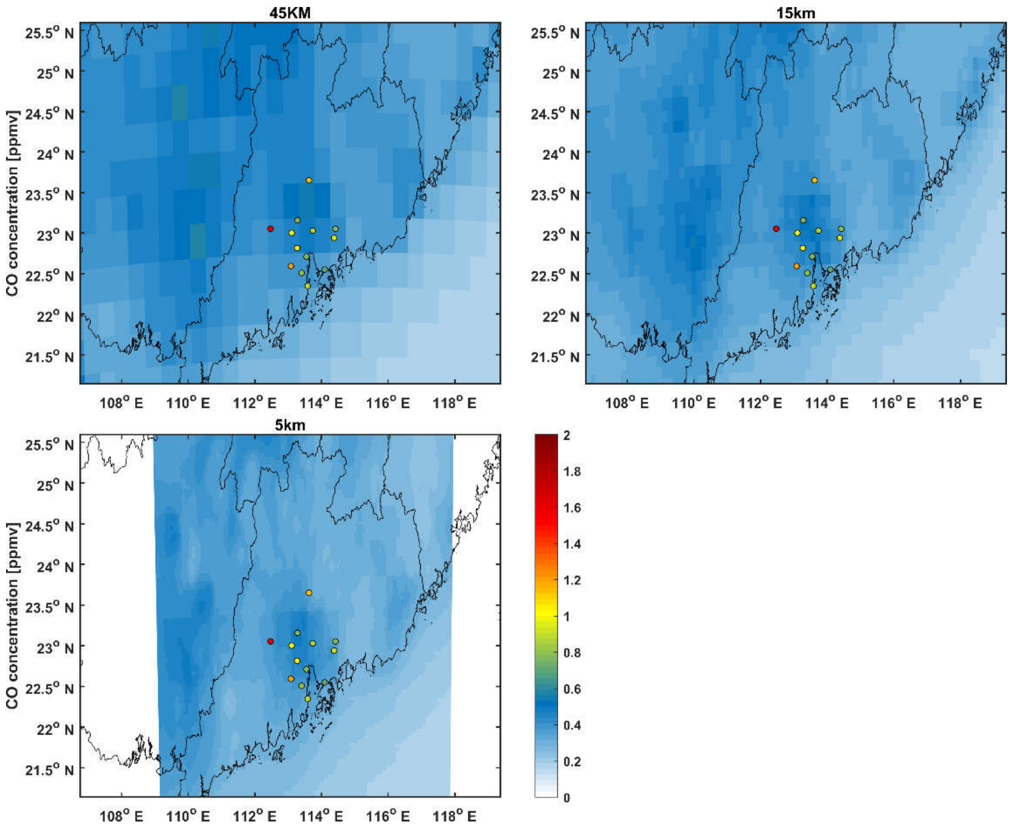

Figure S6: Same as fig.S6 but for CO concentrations.

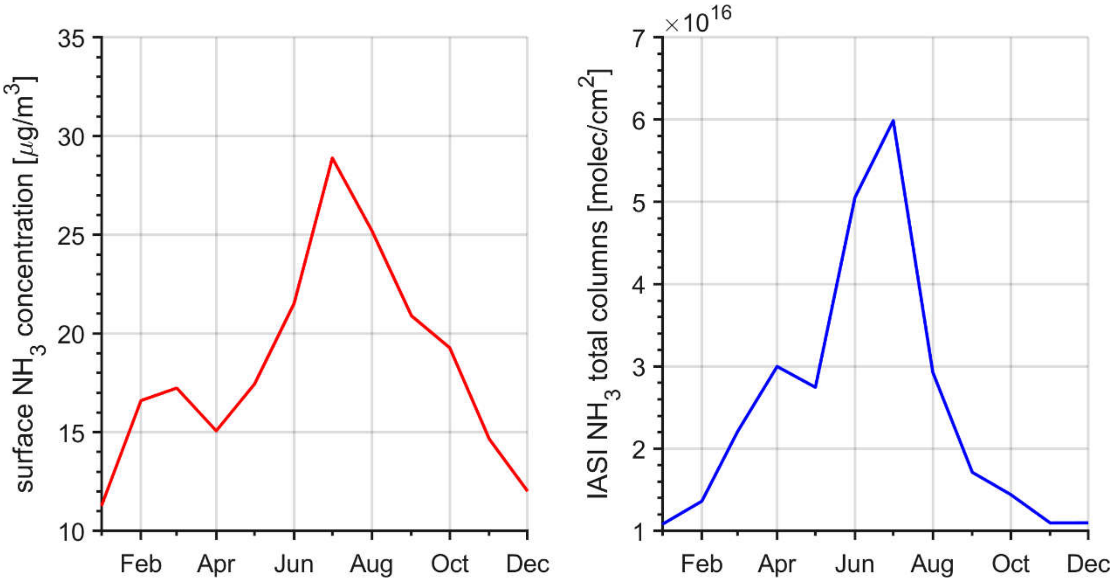

Figure S7: Time series of the surface NH_3 concentrations (left panel) from AMoN-China and NH_3 total columns from IASI (right panel) over the NCP region during September 2015 – August 2016. Note that we reordered the months to better characterise the monthly variations.

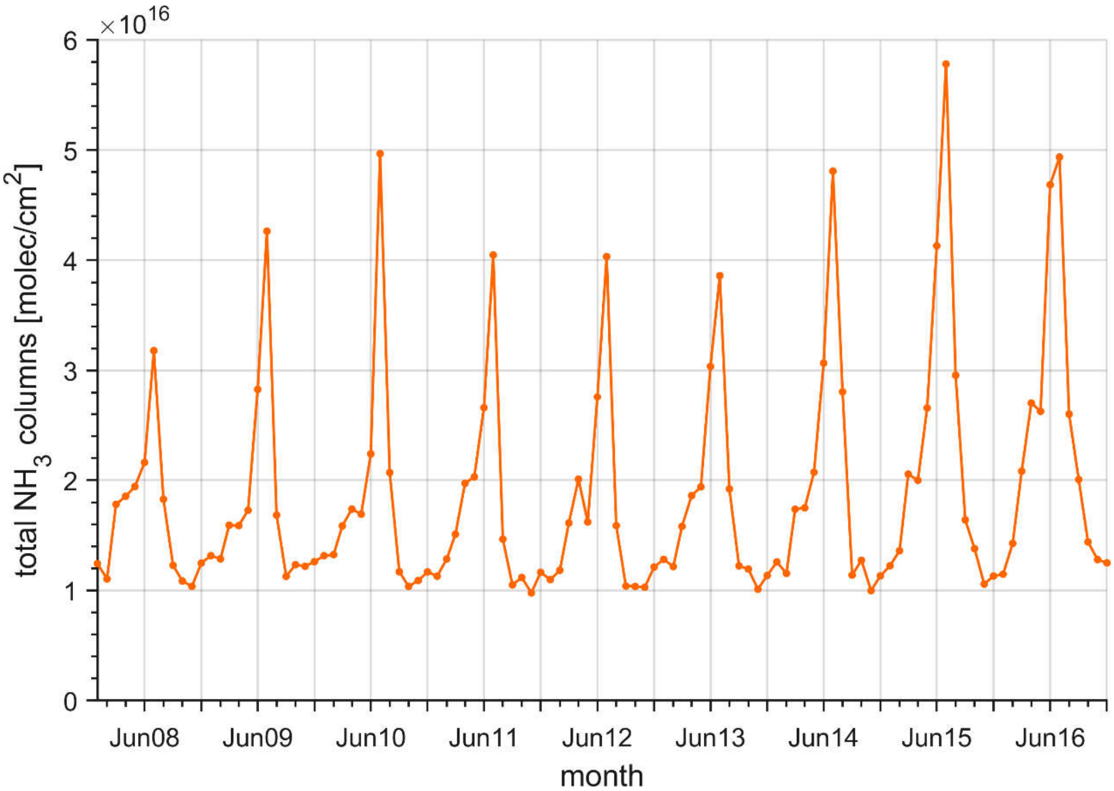

Figure S8: Monthly series of IASI measured NH_3 total columns over the NCP region from year 2008 to 2016

References

Smith, A., Lott, N., and Vose, R.: The Integrated Surface Database Recent Developments and Partnerships, Bull. Amer. Meteorol. Soc., 92, 704-708, 10.1175/2011bams3015.1, 2011.

Van Damme, M., Whitburn, S., Clarisse, L., Clerbaux, C., Hurtmans, D., and Coheur, P. F.: Version 2 of the IASI NH_3 neural network retrieval algorithm: near-real-time and reanalysed datasets, Atmos. Meas. Tech., 10, 4905-4914, 10.5194/amt-10-4905-2017, 2017.

Van Damme, M., Clarisse, L., Whitburn, S., Hadji-Lazaro, J., Hurtmans, D., Clerbaux, C., and Coheur, P.-F.: Level 2 dataset and Level 3 oversampled average map of the IASI/Metop-A ammonia (NH_3) morning column measurements (ANNI-NH3-v2.1R-I) from 2008 to 2016. PANGAEA, 2018.

Whitburn, S., Van Damme, M., Clarisse, L., Bauduin, S., Heald, C. L., Hadji-Lazaro, J., Hurtmans, D., Zondlo, M. A., Clerbaux, C., and Coheur, P. F.: A flexible and robust neural network IASI-NH_3 retrieval algorithm, J. Geophys. Res.-Atmos., 121, 6581-6599, 10.1002/2016jd024828, 2016.